Fingerprinting sediment sources using fallout radionuclides demonstrates that subsoil provides the major source of sediment in sub-humid Ethiopia

Tirusew Abere, Olivier Evrard, Thomas Chalaux-Clergue, Enyew Adgo, Hanibal Lemma, Elie Verleyen, Amaury Frankl

Fingerprinting sediment sources using fallout radionuclides demonstrates that subsoil provides the major source of sediment in sub-humid Ethiopia

Tirusew Abere[1, 2*], Olivier Evrard[3], Thomas Chalaux-Clergue[3], Enyew Adgo[2], Hanibal Lemma[4], Elie Verleyen[5], Amaury Frankl[1]

[1]Department of Geography, Ghent University, Krijgslaan 281 (S8), B-9000 Ghent, Belgium

[2]Department of Natural Resources Management, Bahir Dar University, Bahir Dar 5501, Ethiopia

[3]Laboratoire des Sciences du Climat et de l'Environnement (LSCE), Unité Mixte de Recherche 8212 (CEA-CNRS-UVSQ/IPSL), Gif-sur-Yvette, France

[4]School of Civil and Water Resources Engineering, Bahir Dar University, Bahir Dar 1094, Ethiopia

[5]Department of Biology, Ghent University, Krijgslaan 281 (S8), 9000 Ghent, Belgium

[*]Corresponding author. *Email addresses*: tirusewabere@gmail.com; tirusewabere.chekol@ugent.be

Abstract

Purpose To mitigate erosion, soil and water conservation measures have been introduced widely, with the ambition to reduce on-site erosion rates and catchment sediment yield. However, the success of such measures has been questioned, and often lacks a scientific basis. This is especially true in Ethiopia where gullying has been reported to worsen because of the implementation of soil and water conservation programmes targeting sheet and rill erosion from cropland only. The current research therefore focuses on identifying the sources of sediment based on the dominant erosion processes at play.

Methods This study was conducted in the Fota-Gumara catchment (211 km²), situated in the Lake Tana Basin. The investigation was based on the analysis of fallout radionuclides (^{137}Cs and ^{210}Pb-ex) tracers, which are able to discriminate between topsoil and subsoil. Target material consisted of sediment deposits collected during eight rainfall-runoff events, which occurred in the early and late rainy season of 2023. The activity of ^{137}Cs and ^{210}Pb was measured using gamma spectrometry, while the source apportionment was based on the implementation of Bayesian Models BMM and MixSIAR.

Results Our findings confirmed that subsoil was the major source of sediment. Both models showed consistent results, indicating that approximately three-quarters of the sediment originates from subsoils, contributing a median average of 73% and 81% according to MixSIAR and BMM, respectively. Both the inter-event and seasonal variability of sediment source contributions were relatively low.

Conclusions We conclude that gullies should be a land management priority. Additionally, we demonstrated the validity of using fallout radionuclides for tracing sediment sources in this region of tropical Africa.

Keywords: Soil erosion, Gully, Sediment tracing, Fallout Radionuclides, Lake Tana Basin

1 Introduction

Soil erosion is a major concern affecting soil health globally (Pimentel and Burgess 2013; Borrelli et al. 2021). In order to mitigate erosion, soil and water conservation measures have been introduced, with the aim to reduce on-site erosion rates and catchment sediment yield (Evrard et al. 2016; Rode et al. 2018; Jiang et al. 2020; Huang et al. 2022). Therefore, identifying the location and magnitude of erosion processes is crucial to design effective mitigation strategies (Collins et al. 2001, 2017; Gellis et al. 2019; Evrard et al. 2022; Frankl et al. 2022). In Ethiopia, studying erosion and sediment yield has predominantly focused on sheet and rill erosion, relying on erosion plot data (Ebabu et al. 2023) and soil erosion models (Aga et al. 2018; Lemma et al. 2019; Belay et al. 2020). However, land degradation processes such as gullying, landslides or streambank erosion are often overlooked (Yibeltal et al. 2023). This is in sharp contrast to the observation by numerous studies that such processes play an important role in the loss of soil resources and in the contribution to sediment yield in Ethiopia (Laceby et al. 2015; Huang et al. 2022). For instance, Zegeye et al. (2018) reported that gullies contributed approximately 90% of the sediment in the small Debre Mewi catchment in the sub-humid Ethiopian highlands. Similarly, Yibeltal et al. (2023) reported that gullies were responsible for nearly 85% of the sediment contribution in Aba Gerima catchment in the upper Blue Nile Basin. Elevated sediment yield, which hampers the rural economy and raises environmental concerns (Donohue and Garcia Molinos 2009), has led to the rapid sedimentation of Lake Tana at a rate of 9,800 Mg km^{-2} yr^{-1}, shortening its life expectancy (Lemma et al. 2020). The latter is a major concern for most lakes and reservoirs in Africa (Vanmaercke et al. 2014; Annys and Frankl 2024).

Sediment source fingerprinting is a methodology utilized to identify the provenance of sediment within a given catchment (Walling 2013; Collins et al. 2020; Evrard et al. 2022). Its

specificity lies in the ability to quantify the relative contributions of different sediment source types (Evrard et al. 2022; Vale et al. 2022; Xu et al. 2022). Various tracers have been employed to differentiate between diverse sediment source types (Collins et al. 2020; Evrard et al. 2022). For example, geochemical tracers are commonly used to define which lithological units contribute to sediment mixtures (Akayezu et al. 2020), while fallout radionuclides are used to discern between sediment originating from topsoil erosion (sheet and rill erosion) and subsoil erosion (gullying and streambank) (Haddadchi et al. 2013; Evrard et al. 2016, 2020). Land cover types can also be targeted, using organic matter properties, compound-specific stable isotopes, or environmental DNA (Aliyanta and Sidauruk 2019; Evrard et al. 2019; Frankl et al. 2022). In order to enable the quantification of relative sediment source contributions, a tracer should satisfy two criteria: (1) it should be capable of uniquely identifying and discriminating between potential sediment source types, and (2) it must remain stable (i.e., conservative) during erosion transportation and deposition from source to sink (Collins et al. 2020).

Fallout radionuclides has been widely used as valuable tracers for identifying the origin of sediment in relation to erosion processes (Ben Slimane et al. 2013; Evrard et al. 2020; Foucher et al. 2021). This is because fallout radionuclide activity tends to be elevated in topsoil while being depleted in subsoil (Haddadchi et al. 2013). The most widely used fallout radionuclides for sediment source tracing are excess Lead-210 (^{210}Pb-ex), Caesium-137 (^{137}Cs) and Beryllium-7 (^{7}Be) radioisotopes (Evrard et al. 2020; Foucher et al. 2021). They have been widely employed in sediment fingerprinting research targeting catchments in the Northern hemisphere (Evrard et al. 2020). However, there have been very few studies in the tropics and the Southern hemisphere, specifically in Africa (Evrard et al. 2020). This is due to the concern that the concentration of ^{137}Cs would be too low in these areas as a result of its limited fallout (Evrard et al. 2020) and to the difficult access and the relatively high cost of laboratory analyses (Collins et al. 2017). Despite these concerns research has demonstrated that topsoil and subsoil

may successfully be differentiated based on their ^{137}Cs concentrations in the Southern hemisphere (Rode et al. 2018).

Accordingly, the central question of the current research is to investigate whether the erosion of subsoils provides the major source of sediment in the Lake Tana Basin in Ethiopia, the latter representing an erosion hotspot in Africa. We conducted our investigation in a catchment, which in terms of physiography, land use and land degradation is representative for the wider environment, and explicitly considered seasonal variations when designing the study. In addition to its focus on addressing source contributions to sediment mixtures, we note that sediment source fingerprinting is still a relatively new approach in Ethiopia (e.g., Verheyen et al. 2014; Awoke et al. 2022). To the best of our knowledge, fallout radionuclides have never been employed as tracers in this region. Therefore, we used tracers (^{137}Cs and ^{210}Pb-ex), which have been widely tested and which are capable of discerning topsoil from subsoil, to quantify the respective contribution of erosion processes to sediment. Indeed, sheet and rill erosion, as they only affect the soil surface, contribute topsoil to sediment mixtures. On the contrary, gullying and streambank causes deep incision into the soil, and will predominantly supply subsoil (Fig. 1).

Fig.1 here

2 Materials and Methods

2.1 Study area

The study considers the Fota-Gumara catchment (211 km²; 11°36’ - 11°39’ N, 37°42’ - 38°00’ E; Fig. 2), located in the lake Tana Basin, Ethiopia. Its elevation ranges from 2100 to 2700 meters above sea level, encompassing two agro-ecological zones: midland and highland. The study area experiences a tropical monsoon climate characterized by distinct wet and dry seasons, with the main rainy season occurring from June to September. The annual average rainfall ranges from 1,141 to 1,515 mm, and the daily average air temperature ranges from

9.5°C to 21.8°C (Ayele et al. 2016). According to the Köppen-Geiger climate classification (Peel et al. 2007), the climate of the area is temperate (Cwb type), with dry winters and warm summers. Basalt is the predominant lithology, with some areas covered by volcanic ash (Poppe et al. 2013). The primary soil groups in the study area are Leptosols (36.5%), Luvisols (31%), Nitosols (15%) and Vertisols (5.8%) (ADSWE 2015). Due to high erosion rates, the Fota-Gumara catchment contributes a substantial amount of sediment to Lake Tana, raising significant concerns for land managers (Lemma et al. 2019; Assaye et al. 2021). Of particular concern is the loss of woody vegetation in valley floor areas, which has led to a sharp increase in gullying over recent decades (Frankl et al. 2019).

Fig. 2 here

As shown in Fig. 2, 80% of the study area is occupied by cropland, with the main crops being teff (*Eragrostis tef*), maize (*Zea mays*), barley (*Hordeum vulgare*), wheat (*Triticum aestivum*), finger millet (*Eleusine coracana L.)* and potato (*Solanum tuberosum*) (Assaye et al. 2021). The remaining land consists of shrubland or forest (13%), and comprising built-up areas and severely degraded zones known as “Badlands” (7%).

2.2 Soil and sediment sampling

Prior to this study, areas subjected to severe soil erosion were identified through field observations, participatory mapping and modelling (Abere et al. 2024). This approach allowed for targeting areas experiencing high erosion rates and showing efficient connectivity to drainage channels for sampling. A total of 30 topsoil samples (14 from cropland, eight from grazing land, five from forest and three from shrubland) and 25 subsoil samples (13 from gully walls and 12 from streambanks) were collected. Topsoil was obtained by taking the upper 2 cm of soil from non-cultivated fields and the upper 10 cm from cultivated fields, the latter taking account of soil homogenization due to tillage. Subsoil was collected from actively

eroding gully walls and streambanks and represent the soil below the A-horizon. The soil samples were collected in June and July 2023.

Sediment samples were collected along river at the outlet of the catchment and at two major tributaries. These consider lag deposits, which were collected soon (i.e., within 1 day) after rainfall-runoff events (Laceby et al. 2015). To detect potential seasonal variations in sediment source contributions, samples were obtained both at the beginning and end of the rainy season, capturing shifts in crop phenology and hydro-sedimentological conditions (Lemma et al. 2020). A total of eight sediment samples were collected: five samples at the beginning of the rainy season (26, and 30 June 2023, 04, 06, and 18 July 2023) and three samples at the end (10, 20, and 26 September 2023). All samples correspond to composites, which are a mixture of five to ten sub-samples collected at nearby locations. This improves the representativeness of their properties while minimizing potential effects of local heterogeneity. The samples were collected using a trowel and were sealed in plastic bags. The centroid of the sampling locations serves for their localisation, recorded using a hand-held Global Navigation Satellite System (GNSS).

2.3 Radionuclide analyses

The samples were prepared for radionuclide analyses at the soil laboratory of Bahir Dar University in Ethiopia. They were air-dried and gently disaggregated using a mortar and pestle. Following the recommendations of Evrard et al. (2022), the samples were sieved to 63 µm to keep the fraction to which radionuclides are sorbed to (i.e. silt and clay). The results of this study are therefore directly relevant to understand the sources of suspended sediment. Samples of 20 g (of dry and sieved material) were prepared for radionuclide analysis and placed in airtight polyethylene containers. The activity of the radionuclides ^{137}Cs and ^{210}Pb were measured using gamma spectrometry with low-background N and P type GeHP detectors (Canberra/Ortec) at the Laboratoire des Sciences du Climat et de l'Environnement (Gif-sur-

Yvette, France). Excess ^{210}Pb was calculated by subtracting the supported activity (determined using two 226Ra daughters, ^{214}Pb (average count number at 295.2 and 351.9 keV) and ^{214}Bi (at 609.3 keV)) from the total activity of ^{210}Pb. The results were expressed in Bq kg^{-1}. The measured activities were decay-corrected to the sampling date.

To determine whether fine-grained sources are the major contributors to sediment at the sampled locations, duplicate sediment samples of 25 g were collected and sieved using the wet sieving method. Fractions of sand, silt and clay could be determined using sieves of 63 µm and 2000 µm (Ma et al. 2024).

2.4 Tracer selection and sediment source apportionment

In order to improve the performance of the sediment fingerprinting modelling (Cox et al. 2023), a tracer selection method was applied, which is based on a two-step statistical technique to select conservative and discriminant tracers (Chalaux-Clergue et al. 2024). Initially, a standard range test was applied using the mean plus/minus the standard deviation ("mean ± SD") range test criteria to filter out non-conservative tracers. Then, the two-sample Kolmogorov-Smirnov test was used to select discriminant tracers that can differentiate between sediment derived from topsoil and from subsoil. An α-value of 0.05 was employed to determine the level of significance. We did not apply a discriminant function analysis, as we used a small number of tracers and its application remains a matter of discussion in scientific debates (Du et al. 2019). Smith et al. (2018) also stated that selecting tracers using the Kruskal-Wallis H-test and a discriminant function analysis approach is less accurate and uncertain. Furthermore, Sherriff et al. (2015) emphasize that uncertainty in source predictions can be mitigated by increasing the number of tracers.

The relative contribution of topsoil and subsoil to sediment mixtures were estimated using the following Bayesian mixing models: (1) MixSIAR (Stock et al. 2020, ver. 3.1.12) with JAGS (Stock et al. 2022, ver. 4.3.1), and (2) BMM (Batista et al. 2019) along with the fingR

R-Package (Chalaux-Clergue and Bizeul 2024, ver. 2.1.0). The MixSIAR model is among the most widely used model for sediment source unmixing due to its flexibility (Davies et al. 2018; Du et al. 2019). The MixSIAR model is fitted with a Markov Chain Monte Carlo routine, allowing for a robust estimation of source contributions. The MixSIAR model was run with a very long run type (chain length =1,000,000, burn-in=500,000, thin = 500 and chain = 3) and process error structure (Stock and Semmens 2013, 2016). Similarly, the BMM model was run with 2500 iterations (Batista et al. 2022). The median values of the distribution predicted by both MixSIAR and BMM models were used as the source contributions to the target sediment (Chalaux-Clergue et al. 2024). All statistical analyses were conducted using R-software (R Core Team 2023).

The accuracy of the MixSIAR and BMM models was evaluated using virtual mixtures (Batista et al. 2022; Fathabadi and Jansen 2022; Chalaux-Clergue et al. 2024). For the two source types (topsoil and subsoil), 21 virtual mixtures were generated containing variable source proportions ranging from 0 to 100%, with 5% increments. All mixtures were generated using the fingR version 2.1.0 virtual mixture building function (Chalaux-Clergue and Bizeul 2024). The accuracy of the model predictions was evaluated using following metrics: (1) Continuous Ranked Probability Score (CRPS) for assessing both the accuracy and precision of mixing model predictions (Batista et al. 2022), (2) prediction interval width (W50) to measure model prediction uncertainty (Batista et al. 2022; Chalaux-Clergue et al. 2024), (3) Mean Error (ME) to understand over / under estimation, Root-Mean-Square Error (RMSE) to calculate prediction errors (Chai and Draxler 2014), (4) Pearson correlation coefficient (r^2), and (5) Nash–Sutcliffe Efficiency coefficient (NSE) to understand the performance of the models (Nash and Sutcliffe 1970; Barber et al. 2020; Duc and Sawada 2023).

3 Results

3.1 Grain size and fallout radionuclide properties

Fine texture classes (< 63 µm) dominated grain sizes for all sample types (Fig. 3), with little variability between groups. The sediment samples had an average clay and silt content of 83.6%, which falls within the full range of values represented in the boxplot of the source soil samples. The sand content of all the samples was below 35%, with an average of 15%.

Fig.3 here

The highest specific activity of ^{210}Pb-ex and ^{137}Cs was observed in topsoil from undisturbed forests, followed by topsoil from shrubland, grazing land and cropland. This may be attributed to an elevated organic carbon content and very low soil erosion rates in forest land (Cerdan et al. 2010; Gaspar et al. 2021). Accordingly, soil erosion from forest land was not considered as a potential sediment source in the current research. This is supported by a study conducted by Assaye et al. (2021), who found that the sediment yield from forests was 0.8 Mg ha^{-1} yr^{-1} in the Enkulal catchment, as small sub-catchment of our study area. In contrast, the lowest specific activity of ^{210}Pb-ex and ^{137}Cs was recorded from gullies and streambanks (Fig. 4).

Fig. 4 here

3.2 Tracer selection

Based on the mean ± SD range test criterion, both ^{210}Pb-ex and ^{137}Cs could be considered as conservative tracers (Table 1). Additionally, the non-parametric two-sample Kolmogorov-Smirnov test verified that both ^{210}Pb-ex and ^{137}Cs could differentiate between top- and subsoil sources with a respective p-value of <0.001 and 0.014. Furthermore, the biplot of ^{137}Cs and ^{210}Pb-ex specific activities in Fig. 5 supports the conservative behaviour of these tracers, as the specific activity of the sediment samples was within the range found in the identified source types (i.e. sampled topsoil and subsoil types). Additionally, the violin plots in Fig. 6 also

confirmed that there was indeed a difference between the activities of ^{137}Cs and ^{210}Pb-ex in the top- and subsoil sources and that values found in the target sediment samples were somewhere in-between. This demonstrated that the two tracers could differentiate between the top-and subsoil sources (Derakhshan-Babaei et al. 2024).

Table 1 here

Fig. 5 here

Fig. 6 here

3.3 Mixing models accuracy

The accuracy of both MixSIAR and BMM models was evaluated using several accuracy metrics calculated using virtual mixtures (Table 2). The residual error/bias (ME) was only 2% for MixSIAR and even 0% for BMM, and the root mean square error (RMSE) amounted to 16% for MixSIAR and 5% for BMM. The Pearson's correlation coefficient (r^2) and the Nash-Sutcliffe efficiency (NSE) were high for BMM model and slightly lower for MixSIAR. Although there is no defined threshold for W50* values, the results suggested a somewhat elevated uncertainty for both models, with 21.6% for MixSIAR and 37.5% for BMM. The CRPS values were low for both models, as they remained below 9%.

Table 2 here

3.4 Contribution of top- and subsoil to sediment yield

The dominance of subsoil contribution to sediment mixtures indicates that gullying and streambank erosion are the major processes contributing to sediment yield in the study area for the considered events. Both MixSIAR and BMM models showed consistent results, indicating that about three-quarters of the sediment originates from erosion processes exposing subsoils. The median contribution of subsoil to sediment mixtures ranged from 67% (95% credible interval: 22%–86%) to 77% (95% credible interval: 28%–93%) according to MixSIAR, and from 76% (95% credible interval: 0.1%–99.9%) to 92% (95% credible interval: 0.1%–99.9%)

according to BMM. The central values (or average of the medians) of the subsoil contribution to sediment mixtures were 73% (95% credible interval: 20%–80%) for MixSIAR and 81% (95% credible interval: 0.1%–99.9%) for BMM (Fig. 7).

Fig.7 here

For all investigated rainfall-runoff events, subsoil remained the major contributor to sediment mixtures, albeit minor variability between events (Fig. 8). Consequently, sampling sediment that deposited both during the early and late rainy seasons did not support the hypothesis that evidence of the occurrence of changes in the sediment contributions between the two source types.

Fig. 8 here

4 Discussion

4.1 Validity of using fallout radionuclides as tracers

The proportion of clay and silt in the sediment matched that of the soils (Fig. 3), indicating that fine sediment sources dominate sediment yield in the catchment. As fallout radionuclides mainly bind to fine fractions (Evrard et al. 2020), these results support the validity of the approach (applied to <63 µm fractions of material). In the nearby river, the bedload contribution to total sediment yield was quantified to 0.1 to 5.4% (Lemma et al. 2019), which is consistent with our findings. This is also supported by Kebedew et al. (2020), who found 88% of fine fractions in the sediment of lake Tana.

Both ^{210}Pb-ex and ^{137}Cs were conservative and discriminant tracers, able to distinguish topsoil from subsoil (Table 1). This finding opens new avenues for future research in the wider region, as it demonstrates that, even though the activity of ^{137}Cs is rather low in the tropics, it remains sufficiently elevated and thus valid for implementing sediment fingerprinting. Rode

et al. (2018) also reported that fallout radionuclide tracers (^{210}Pb-ex and ^{137}Cs) were applicable to differentiate topsoil and subsoil as sediment sources in Burkina Faso.

Evaluating the MixSIAR and BMM models using virtual mixtures indicated a good performance for apportioning sediment sources (Table 2). For both models, the ME and CRPS values align with those reported by Batista et al. (2022), who found a ME value of less than 4% and a CRPS value of 9%. The RMSE values for MixSIAR were nearly similar with the findings of Chalaux-Clergue et al. (2024), who reported an average RMSE value of 14%, while these values were lower for BMM. However, the W50* values for both models were a slightly higher than those reported by Chalaux-Clergue et al. (2024), who found an average W50* value of 11%. Although the prediction uncertainty was higher for BMM, it was comparable to that reported by Batista et al. (2022). Additionally, the performance (NSE) of BMM exceeded that of MixSIAR, also aligning with the findings of Batista et al. (2022).

The specific activity of ^{137}Cs was generally low in both the top- and subsoil samples and below the detection limit in the sediment samples. However, there is a notable difference in its activity between the top- and subsoil sources at a p-value of 0.014. The specific activity of ^{210}Pb-ex was high in the topsoil, low in the subsoil, and intermediate in the sediment samples (Fig. 6). The specific activities of both tracers were nearly similar to the findings reported by Ben Slimane et al. (2013) in Tunisia (South Africa), Rode et al. (2018) in Burkina Faso (West Africa), Evrard et al. (2010, 2016) in central Mexico and Northern Laos, respectively. For long-term tracing in this region, it is likely better to rely on natural radionuclides such as ^{210}Pb-ex, as ^{137}Cs will inexorably continue to decay without being replenished (FAO 2014; Evrard et al. 2020). This is because natural radionuclides are continuously supplied through rainfall, in contrast to artificial ^{137}Cs, which was exclusively emitted during nuclear activities (Prăvălie 2014).

4.2 Subsoil as the major source of sediment

309 The central question of this work was to investigate whether the erosion of subsoils provides
310 the major source of sediment in the Lake Tana Basin in Ethiopia, allowing to support our
311 hypothesis that gullying is a major land degradation issue. Through investigating a medium-
312 sized catchment (211 km²) and taking the variability between individual events and seasonal
313 trends into account, this paper confirms that subsoils supplied the vast majority of sediment to
314 rivers in the catchment. Similarly, Cheng et al. (2020) reported that subsoils contributed to 62%
315 of the sediment in Southwestern China. Rode et al. (2018) and Evrard et al. (2016) also noted
316 that subsoils were a primary contributor to sediment mixtures in respectively Burkina Faso and
317 Laos. Based on extensive field surveys and previous research, gullying had been identified as
318 a major erosion problem in the study area (Abere et al. 2024), which also efficiently conveys
319 sediment from hillslopes to channels (Astuti et al. 2024). Gully erosion is widely recognized
320 as a major driver of land degradation in the region (Frankl et al. 2013; De Geeter et al. 2023).
321 For example, case studies such as that of Tebebu et al. (2010) report that gully erosion rates
322 were nearly 20 times higher than the sheet and rill erosion rates in Debre Mewi catchment in
323 Ethiopia. This calls for interdisciplinary approaches to improve the effectiveness of land
324 management considering gully erosion (Frankl et al. 2016; Blake et al. 2018; Frankl et al.
325 2019). Streambank erosion is less important in the investigated catchment, with the majority
326 of the river network have low to medium energy floodplains where sedimentation rates can be
327 high (Awoke et al. 2022). Similar findings have been highlighted for other areas in the world,
328 stressing that gullying is a major, but often overlooked concerns. This aligns with the synthesis
329 of Poesen et al. (2003), which pointed to gullying as a major contributor to catchment sediment
330 yield, particularly in the tropics (see relevant reference for Ethiopia in the introduction). In
331 contrast, the sediment provenance from sheet and rill erosion was rather limited (Fig. 7). Recent
332 land management efforts have indeed focussed on limiting soil erosion from cropland, through

the implementation of soil and water conservation measures on steep slopes (Abere et al. 2024; Fenta et al. 2024), which limits sediment mobilization processes (Berihun et al. 2020).

Considering the seasonality in sediment source contributions, it is typically assumed that topsoil input to sediment mixtures is elevated at the beginning of the rainy season. This increase is due to soil exposure during the early cropping phase and the initial flush of loose sediment after the long dry season. Conversely, topsoil erosion is expected to decrease in the late rainy season, as dense crop cover protects the soil from sheet and rill erosion. This study found no evidence of seasonality in sediment sources, challenging the previously held assumption. In the Enkulal sub-catchment, Assaye et al. (2021) reported that runoff and sediment yield from zero-order catchments are largely determined by rainfall characteristics at the event scale. These rainfall-runoff event characteristics significantly influence erosion processes and sediment mobilization (Poleto et al. 2009). Multiple factors may contribute to the lack of seasonality, such as sediment dynamics being transport-limited in the early rainy season (Tilahun 2012), or the high infiltration rates which occur on steep slopes, and where infiltration-excess Hortonian flow has been reported in only 3 to 9% of rainfall events (Bayabil et al. 2010; Tilahun et al. 2016). Such findings, which do not necessarily fit the conceptualizations of hydrogeomorphic responses, have been obtained in other regions of the world too, for example in Ireland by Sherriff et al. (2018) and in the Northern Loess Plateau, China by Tian et al. (2023).

5 Conclusions

This paper highlights that subsoils provides the major source of sediment in the Lake Tana Basin in Ethiopia, allowing to support our hypothesis that gullying is a major land degradation issue. This finding is based on the first application of sediment fingerprinting using fallout radionuclides in sub-humid Ethiopia. Models provided consistent results, indicating that about three-quarters of the sediment originates from subsoils (median average of 73% for MixSIAR and 81% for BMM). We conclude that ^{137}Cs and ^{210}Pb-ex proved to be effective tracers for distinguishing between topsoil and subsoil contributions to sediment mixtures in Ethiopia. Among the two, ^{210}Pb-ex performed better, offering a more sustainable, long-term solution given the continuous decay of ^{137}Cs. The accuracy of MixSIAR and BMM models for apportioning topsoil and subsoil sediment source contributions were high. While the performance of BMM was higher than MixSIAR, the latter provided greater certainty. Both inter-event and seasonal variability in sediment contribution remained limited. Accordingly, land managers should prioritize gullies when aiming to control excessive sediment yield in the Lake Tana Basin, instead of primarily focussing on sheet and rill erosion on cropland.

Acknowledgements This study was supported by the Special Research Fund of Ghent University (Grant code: BOF.DCV.2022.0003). The fieldwork was partially funded by the VLIR-UOS funded BDU-IUC Phase 2 Project (UOS.IUS.2023.0001.01). We thank Deribew Fentie, Solomon Afework, and Abebe for their support during fieldwork.

Declarations

Conflict of interest: The authors declared that there is no competing interests.

References

ADSWE (2015) Amhara National Regional State Bureau of Environmental Protection, Land Administration and Use, Tana sub basin land use planning and environmental study project technical report: Implementation guideline (ADSWE , LUPESP / TaSB : Section III Volume VI/. 058. ANRS BoEPLAU, Bahir Dar, Ethiopia. https://mahiderzewdie.wordpress.com/wp-content/uploads/2015/08/tosb_sea-apprisal

Aga AO, Chane B, Melesse AM (2018) Soil erosion modelling and risk assessment in data scarce Rift Valley Lake regions, Ethiopia. Water 10:1–17. https://doi.org/10.3390/w10111684

Akayezu P, Musinguzi L, Natugonza V, Ogutu-Ohwayo R, Mwathe K, Dutton C, Manyifika M (2020) Using sediment fingerprinting to identify erosion hotspots in a sub-catchment of Lake Kivu, Rwanda. Environ Monit Assess 192:1–15. https://doi.org/10.1007/s10661-020-08774-5

Aliyanta B, Sidauruk P (2019) Sediment sources analysis using CSSI method in Pasir Buncir micro-watershed, Bogor, Indonesia. Atom Indonesia 45:89–95. https://doi.org/10.17146/aij.2019.721

Ankers C, Walling DE, Smith RP (2003) The influence of catchment characteristics on suspended sediment properties. Hydrobiologia 494:159–167. https://doi.org/10.1023/A:1025458114068

Assaye H, Nyssen J, Poesen J, Lemma H, Meshesha DT, Wassie A, Adgo E, Fentie D, Frankl A (2021) Event-based run-off and sediment yield dynamics and controls in the subhumid headwaters of the Blue Nile, Ethiopia. Land Degrad Dev 33:565–580. https://doi.org/10.1002/ldr.4144

Astuti AJD, Dondeyne S, Lemma H, Nyssen J, Annys S, Frankl A (2024) Recent dynamics in sediment connectivity in the Ethiopian Highlands. Reg Environ Change 24:1–14. https://doi.org/10.1007/s10113-024-02277-6

Awoke GW, Brees J, Vancampenhout K, Adgo E, Abate M, Wassie A, Frankl A, Verstraeten G (2022) Factors controlling floodplain sediment storage in two tropical upland river catchments in the Lake Tana basin, Ethiopia. Catena 219:1–15. https://doi.org/10.1016/j.catena.2022.106573

Awoke GW, Verstraeten G, Vancampenhout K, Boeckx P (2022) Floodplain sedimentation history and source apportionment for tropical mountainous river catchments in the Lake Tana Basin, NW Ethiopia. PhD dissertation, KU Leuven. https://research.kuleuven.be/portal/en/project/3E170785

Ayele HS, Li MH, Tung CP, Liu TM (2016) Assessing climate change impact on Gilgel Abbay and Gumara watershed hydrology, the upper blue Nile basin, Ethiopia. Terr Atmos Ocean Sci 27:1005–1018. https://doi.org/10.3319/tao.2016.07.30.01

Barber C, Lamontagne JR, Vogel RM (2020) Improved estimators of correlation and R^2 for skewed hydrologic data. Hydrol Sci J 65:87–101. https://doi.org/10.1080/02626667.2019.1686639

Batista PVG, Laceby JP, Evrard O (2022) How to evaluate sediment fingerprinting source apportionments. J Soils Sediments 22:1315–1328. https://doi.org/10.1007/s11368-022-03157-4

Batista P G, Laceby JP, Silva MLN, Tassinari D, Bispo DFA, Curi N, Davies J, Quinton JN

(2019) Using pedological knowledge to improve sediment source apportionment in tropical environments. J Soils Sediments 19:3274–3289. https://doi.org/10.1007/s11368-018-2199-5

Bayable HK, Tilahun SA, Amy S, Collick BY, Steenhuis TS (2010) Are runoff processes ecologically or topographically driven in the (sub) humid Ethiopian highlands? The case of the Maybar watershed. Ecohydrol 130:126–130. https://doi.org/10.1002/eco

Ben Slimane A, Raclot D, Evrard O, Sanaa M, Lefèvre I, Ahmadi M, Tounsi M, Rumpel C, Ben Mammou A, Le Bissonnais Y (2013) Fingerprinting sediment sources in the outlet reservoir of a hilly cultivated catchment in Tunisia. J Soils Sediments 13:801–815. https://doi.org/10.1007/s11368-012-0642-6

Belay HT, Malede DA, Geleta FB (2020) Erosion risk potential assessment using GIS and RS for soil and water resource conservation plan: The case of Yisir watershed, Northwestern Ethiopia. Agric For Fish 9:1–13. https://doi.org/10.11648/j.aff.20200901.11

Berihun ML, Tsunekawa A, Haregeweyn N, Dile YT, Tsubo M, Fenta AA, Meshesha DT, Ebabu K, Sultan D, Srinivasan R (2020) Evaluating runoff and sediment responses to soil and water conservation practices by employing alternative modeling approaches. Sci Total Environ 747:1–19. https://doi.org/10.1016/j.scitotenv.2020.141118

Blake WH, Rabinovich A, Wynants M, Kelly C, Nasseri M, Ngondya I, Patrick A, Mtei K, Munishi L, Boeckx P, Navas A, Smith HG, Gilvear D, Wilson G, Roberts N, Ndakidemi P (2018) Soil erosion in East Africa: An interdisciplinary approach to realising pastoral land management change. Environ Res Letters 13:1–12. https://doi.org/10.1088/1748-9326/aaea8b

Borrelli P, Alewell C, Alvarez P, Anache JAA, Baartman J, Ballabio C, Bezak N, Biddoccu M, Cerdà A, Chalise D, Chen S, Chen W, De Girolamo AM, Gessesse GD, Deumlich D, Diodato N, Efthimiou N, Erpul G, Fiener P, Panagos P (2021) Soil erosion modelling: A global review and statistical analysis. Sci Total Environ 780:1–18. https://doi.org/10.1016/j.scitotenv.2021.146494

Cerdan O, Govers G, Le Bissonnais Y, Van Oost K, Poesen J, Saby N, Gobin A, Vacca A, Quinton J, Auerswald K, Klik A, Kwaad FJPM, Raclot D, Ionita I, Rejman J, Rousseva S, Muxart T, Roxo MJ, Dostal T (2010) Rates and spatial variations of soil erosion in Europe: A study based on erosion plot data. Geomorphol 122:167–177. https://doi.org/10.1016/j.geomorph.2010.06.011

Chai T, Draxler RR (2014) Root mean square error (RMSE) or mean absolute error (MAE)? - Arguments against avoiding RMSE in the literature. Geosci Model Dev 7:1247–1250. https://doi.org/10.5194/gmd-7-1247-2014

Chalaux-Clergue T, Bizeul R (2024) fingR: A package to support sediment source fingerprinting studies, Zenodo: https://doi.org/10.5281/zenodo.8293595, Github: https://github.com/tchalauxclergue/fingR, Version = 2.1.0

Chalaux-Clergue T, Bizeul R, Batista PVG, Martínez-Carreras N, Laceby JP, Evrard O (2024) Sensitivity of source sediment fingerprinting to tracer selection methods. Soil 10:109–138. https://doi.org/10.5194/soil-10-109-2024

Cheng Q, Wang S, Peng T, Cao L, Zhang X, Buckerfield SJ, Zhang Y, Collins AL (2020) Sediment sources, soil loss rates and sediment yields in a Karst plateau catchment in Southwest China. Agric Ecosyst Environ 304:1–11.

https://doi.org/10.1016/j.agee.2020.107114
Collins AL, Blackwell M, Boeckx P, Chivers CA, Emelko M, Evrard O, Foster I, Gellis A, Gholami H, Granger S, Harris P, Horowitz AJ, Laceby JP, Martinez-Carreras N, Minella J, Mol L, Nosrati K, Pulley S, Silins U, Zhang Y (2020) Sediment source fingerprinting: benchmarking recent outputs, remaining challenges and emerging themes. J Soils Sediments 20:4160–4193. https://doi.org/10.1007/s11368-020-02755-4
Collins AL, Pulley S, Foster IDL, Gellis A, Porto P, Horowitz AJ (2017) Sediment source fingerprinting as an aid to catchment management: A review of the current state of knowledge and a methodological decision-tree for end-users. J Environ Manag 194:86–108. https://doi.org/10.1016/j.jenvman.2016.09.075
Collins AL, Walling DE, Sichingabula HM, Leeks GJL (2001) Suspended sediment source fingerprinting in a small tropical catchment and some management implications. Appl Geogr 21:387–412. https://doi.org/10.1016/S0143-6228(01)00013-3
Cox T, Laceby JP, Roth T, Alewell C (2023) Less is more? A novel method for identifying and evaluating non-informative tracers in sediment source mixing models. J Soils Sediments 23:3241–3261. https://doi.org/10.1007/s11368-023-03573-0
Davies J, Olley J, Hawker D, McBroom J (2018) Application of the Bayesian approach to sediment fingerprinting and source attribution. Hydrol Process 32:3978–3995. https://doi.org/10.1002/hyp.13306
De Geeter S, Verstraeten G, Poesen J, Campforts B, Vanmaercke M (2023) A data driven gully head susceptibility map of Africa at 30 m resolution. Environ Res 224: 1–16 . https://doi.org/10.1016/j.envres.2023.115573
Derakhshan-Babaei F, Nosrati K, Fiener P, Egli M, Collins AL (2024) Source fingerprinting sediment loss from sub-catchments and topographic zones using geochemical tracers and weathering indices. J Hydrol 633:1–16. https://doi.org/10.1016/j.jhydrol.2024.131019
Donohue I, Garcia Molinos J (2009) Impacts of increased sediment loads on the ecology of lakes. Biol Rev 84:517–531. https://doi.org/10.1111/j.1469-185X.2009.00081.x
Du P, Huang D, Ning D, Chen Y, Liu B, Wang J, Xu J (2019) Application of Bayesian model and discriminant function analysis to the estimation of sediment source contributions. Int J Sediment Res 34:577–590. https://doi.org/10.1016/j.ijsrc.2019.05.005
Duc L, Sawada Y (2023) A signal-processing-based interpretation of the Nash-Sutcliffe efficiency. Hydrol Earth Syst Sci 27:1827–1839. https://doi.org/10.5194/hess-27-1827-2023
Ebabu K, Taye G, Tsunekawa A, Haregeweyn N, Adgo E, Tsubo M, Fenta AA, Meshesha D T, Sultan D, Aklog D, Admasu T, van Wesemael B, Poesen J (2023) Land use, management and climate effects on runoff and soil loss responses in the highlands of Ethiopia. J Environ Manag 326:1–14. https://doi.org/10.1016/j.jenvman.2022.116707
Evrard O, Batista PVG, Company J, Dabrin A, Foucher A, Frankl A, García-Comendador J, Huguet A, Lake N, Lizaga I, Martínez-Carreras N, Navratil O, Pignol C, Sellier V (2022) Improving the design and implementation of sediment fingerprinting studies: summary and outcomes of the TRACING 2021 Scientific School. J Soils Sediments 22:1648–1661. https://doi.org/10.1007/s11368-022-03203-1
Evrard O, Chaboche PA, Ramon R, Foucher A, Laceby JP (2020) A global review of sediment source fingerprinting research incorporating fallout radiocesium (137Cs). Geomorphol

362:1–22. https://doi.org/10.1016/j.geomorph.2020.107103
Evrard O, Laceby JP, Ficetola GF, Gielly L, Huon S, Lefèvre I, Onda Y, Poulenard J (2019) Environmental DNA provides information on sediment sources: A study in catchments affected by Fukushima radioactive fallout. Sci Total Environ 665:873–881. https://doi.org/10.1016/j.scitotenv.2019.02.191
Evrard O, Laceby JP, Huon S, Lefèvre I, Sengtaheuanghoung O, Ribolzi O (2016) Combining multiple fallout radionuclides (137Cs, 7Be, 210Pbxs) to investigate temporal sediment source dynamics in tropical, ephemeral riverine systems. J Soils Sediments 16:1130–1144. https://doi.org/10.1007/s11368-015-1316-y
Evrard O, Némery J, Gratiot N, Duvert C, Ayrault S, Lefèvre I, Poulenard J, Prat C, Bonté P, Esteves M (2010) Sediment dynamics during the rainy season in tropical highland catchments of central Mexico using fallout radionuclides. Geomorphol 124:42–54. https://doi.org/10.1016/j.geomorph.2010.08.007
FAO (2014) Guidelines for Using Fallout Radionuclides to Assess Erosion and Effectiveness of Soil Conservation Strategies. IAEA Vienna, Austria. https://www.iaea.org/publications/10501
Fathabadi A, Jansen JD (2022) Quantifying uncertainty of sediment fingerprinting mixing models using frequentist and Bayesian methods: A case study from the Iranian loess Plateau. Catena 217:1–12. https://doi.org/10.1016/j.catena.2022.106474
Fenta HM, Aynalem DW, Malmquist L, Haileslassie A, Tilahun SA, Barron J, Adem AA, Adimassu Z, Zimale FA, Steenhuis TS (2024) A critical analysis of soil (and water) conservation practices in the Ethiopian Highlands: Implications for future research and modeling. Catena 234:1–19. https://doi.org/10.1016/j.catena.2023.107539
Foucher A, Chaboche PA, Sabatier P, Evrard O (2021) A worldwide meta-analysis (1977–2020) of sediment core dating using fallout radionuclides including 137Cs and 210Pbxs. Earth Syst Sci Data Discuss 13:4951–4966. https://doi.org/https://doi.org/10.5194/essd-13-4951-2021
Frankl A, Evrard O, Cammeraat E, Tytgat B, Verleyen E, Stokes A (2022) Tracing hotspots of soil erosion in high mountain environments: how forensic science based on plant eDNA can lead the way. An opinion. Plant Soil 476:729–742. https://doi.org/10.1007/s11104-021-05261-9
Frankl A, Nyssen J, Adgo E, Wassie A, Scull P (2019) Can woody vegetation in valley bottoms protect from gully erosion? Insights using remote sensing data (1938–2016) from subhumid NW Ethiopia. Reg Environ Change 19:2055–2068. https://doi.org/10.1007/s10113-019-01533-4
Frankl A, Deckers J, Moulaert L, Van Damme A, Haile M, Poesen J, Nyssen J (2016) Integrated solutions for combating gully erosion in areas prone to soil piping: Innovations from the drylands of Northern Ethiopia. Land Degrad Dev 27:1797–1804. https://doi.org/10.1002/ldr.2301
Frankl A, Poesen J, Haile M, Deckers J, Nyssen J (2013) Quantifying long-term changes in gully networks and volumes in dryland environments: The case of Northern Ethiopia. Geomorphology 201:254–263. https://doi.org/10.1016/j.geomorph.2013.06.025
Gaspar L, Lizaga I, Navas A (2021) Spatial distribution of fallout and lithogenic radionuclides controlled by soil carbon and water erosion in an agroforestry South-Pyrenean catchment. Geoderma 391:1–12. https://doi.org/10.1016/j.geoderma.2021.114941

559 Gellis AC, Fuller CC, Van Metre P, Filstrup CT, Tomer MD, Cole KJ, Sabitov TY (2019)
560 Combining sediment fingerprinting with age-dating sediment using fallout radionuclides
561 for an agricultural stream, Walnut Creek, Iowa, USA. J Soils Sediments 19:3374–3396.
562 https://doi.org/10.1007/s11368-018-2168-z
563 Gellis AC, Gorman Sanisaca L (2018) Sediment fingerprinting to delineate sources of sediment
564 in the agricultural and forested Smith Creek watershed, Virginia, USA. J Am Water
565 Resour Assoc 54:1197–1221. https://doi.org/10.1111/1752-1688.12680
566 Guan Y, Cui L, Huang C, Guo Z, Fan K, Wang H, He H, Wang D, Liu Z (2024) Migration of
567 fallout radionuclides and soil erosion of Hongsongwa mountainous in China.
568 https://doi.org/10.1021/acsearthspacechem.3c00358
569 Haddadchi A, Ryder DS, Evrard O, Olley J (2013) Sediment fingerprinting in fluvial systems:
570 Review of tracers, sediment sources and mixing models. Int J Sediment Res 28:560–578.
571 https://doi.org/10.1016/S1001-6279(14)60013-5
572 Huang D, Du P, Wang J, Wei X, Liu B, Xu J (2019) Using reservoir deposits to quantify the
573 source contributions to the sediment yield in the Black Soil Region, Northeast China,
574 based on the fingerprinting technique. Geomorphol 339:1–18.
575 https://doi.org/10.1016/j.geomorph.2019.04.005
576 Huang D, Su L, Zhou L, Fan H (2022) Gully is the dominant sediment source of snowmelt
577 erosion in the black soil region – A case study. Soil Tillage Res 215:1–11.
578 https://doi.org/10.1016/j.still.2021.105232
579 Jiang G, Lutgen A, Mattern K, Sienkiewicz N, Kan J, Inamdar S (2020) Streambank legacy
580 sediment contributions to suspended sediment-bound nutrient yields from a mid-Atlantic,
581 Piedmont watershed. J Am Water Resour Assoc 56:820–841.
582 https://doi.org/10.1111/1752-1688.12855
583 Kebedew MG, Tilahun SA, Zimale FA, Steenhuis TS (2020) Bottom sediment characteristics
584 of a tropical lake: Lake Tana, Ethiopia. Hydrology 7:1–14.
585 Laceby JP, Olley J, Pietsch TJ, Sheldon F, Bunn SE (2015) Identifying subsoil sediment
586 sources with carbon and nitrogen stable isotope ratios. Hydrol Process 29:1956–1971.
587 https://doi.org/10.1002/hyp.10311
588 Lemma H, Frankl A, Dessie M, Poesen J, Adgo E, Nyssen J (2020) Consolidated sediment
589 budget of Lake Tana, Ethiopia (2012–2016). Geomorphol 371:1–15.
590 https://doi.org/10.1016/j.geomorph.2020.107434
591 Lemma H, Frankl A, van Griensven A, Poesen J, Adgo E, Nyssen J (2019) Identifying erosion
592 hotspots in Lake Tana Basin from a multisite Soil and Water Assessment Tool validation:
593 Opportunity for land managers. Land Degrad Dev 30:1449–1467.
594 https://doi.org/10.1002/ldr.3332
595 Lemma H, Nyssen J, Frankl A, Poesen J, Adgo E, Billi P (2019) Bedload transport
596 measurements in the Gilgel Abay River, Lake Tana Basin, Ethiopia. J Hydrol 577:1–15.
597 https://doi.org/10.1016/j.jhydrol.2019.123968
598 Lizaga I, Gaspar L, Blake WH, Latorre B, Navas A (2019) Fingerprinting changes of source
599 apportionments from mixed land uses in stream sediments before and after an exceptional
600 rainstorm event. Geomorphol 341:216–229.
601 https://doi.org/10.1016/j.geomorph.2019.05.015
602 Ma S, Song Y, Liu J, Kang X, Yue ZQ (2024) Extended wet sieving method for determination

of complete particle size distribution of general soils. J Rock Mech Geotech Eng 16:242–257. https://doi.org/10.1016/j.jrmge.2023.03.006

Munoz-Arcos E, Millward G, Clason C, Bravo-Linares C, Blake W (2023) Variability of fallout radionuclides in river channels: Implications for sediment residence time estimations, EGU General Assembly 2023, Vienna, Austria, 24–28 Apr 2023, EGU23-15828, https://doi.org/10.5194/egusphere-egu23-15828

Nash JE, Sutcliffe JV (1970) River flow forecasting through conceptual models part I - A discussion of principles. J Hydrol 10:282–290. https://doi.org/10.1016/0022-1694(70)90255-6

Peel MC, Finlayson BL, McMahon TA (2007) Updated world map of the K¨oppen-Geiger climate classification. Hydrol Earth Syst Sci 11:1633–1644. https://doi.org/10.1002/ppp.421

Pimentel D, Burgess M (2013) Soil erosion threatens food production. Agriculture 3:443–463. https://doi.org/10.3390/agriculture3030443

Poesen J, Nachtergaele J, Verstraeten G, Valentin C (2003) Gully erosion and environmental change: Importance and research needs. Catena 50:91–133. https://doi.org/10.1016/S0341-8162(02)00143-1

Poleto C, Merten GH, Minella JP (2009) The identification of sediment sources in a small urban watershed in southern Brazil: An application of sediment fingerprinting. Environ Technol 30:1145–1153. https://doi.org/10.1080/09593330903112154

Poppe L, Frankl A, Poesen J, Admasu T, Dessie M, Adgo E, Deckers J, Nyssen J (2013) Geomorphology of the Lake Tana basin, Ethiopia. J Map 9:431–437. https://doi.org/10.1080/17445647.2013.801000

Prăvălie R (2014) Nuclear weapons tests and environmental consequences: A global perspective. Ambio 43:729–744. https://doi.org/10.1007/s13280-014-0491-1

Rode M, op de Hipt F, Collins AL, Zhang Y, Theuring P, Schkade UK, Diekkrüger B (2018) Subsurface sources contribute substantially to fine-grained suspended sediment transported in a tropical West African watershed in Burkina Faso. Land Degrad Dev 29: 4092–4105. https://doi.org/10.1002/ldr.3165

Sherriff SC, Rowan JS, Fenton O, Jordan P, Ó hUallacháin D (2018) Sediment fingerprinting as a tool to identify temporal and spatial variability of sediment sources and transport pathways in agricultural catchments. Agric Ecosyst Environ 267:188–200. https://doi.org/10.1016/j.agee.2018.08.023

Sherriff SC, Franks SW, Rowan JS, Fenton O, Ó'hUallacháin D (2015) Uncertainty-based assessment of tracer selection, tracer non-conservativeness and multiple solutions in sediment fingerprinting using synthetic and field data. J Soils Sediments 15:2101–2116. https://doi.org/10.1007/s11368-015-1123-5

Smith HG, Karam DS, Lennard AT (2018) Evaluating tracer selection for catchment sediment fingerprinting. J Soils Sediments 18:3005–3019. https://doi.org/10.1007/s11368-018-1990-7

Stock BC, Semmens BX (2013) MixSIAR GUI user manual. *Version 3.1*, *March*, 1–42. https://doi.org/10.5281/zenodo.47719.1

Stock BC, Semmens BX (2016) Unifying error structures in commonly used biotracer mixing models. Ecology 97:2562–2569

Stock BC, Jackson AL, Ward EJ, Parnell AC, Phillips DL (2020) MixSIAR: Bayesian Mixing Models in R (Version 3.1.12). Zenodo. https://doi.org/10.5281/zenodo.594910. Github. https://github.com/brianstock/MixSIAR/tree/3.1.11

Stock BC, Semmens BX, Ward EJ, Parnell AC, Phillips DL (2022) JAGS: Bayesian Mixing Models in R, Zenodo [code], https://doi.org/10.5281/zenodo.1209993

Tebebu TY, Abiy AZ, Zegeye AD, Dahlke HE, Easton ZM, Tilahun SA, Collick AS, Kidnau S, Moges S, Dadgari F, Steenhuis TS (2010) Surface and subsurface flow effect on permanent gully formation and upland erosion near Lake Tana in the northern highlands of Ethiopia. Hydrol Earth Syst Sci 14:2207–2217. https://doi.org/10.5194/hess-14-2207-2010

Tebebu TY, Steenhuis TS, Dagnew DC, Guzman CD, Bayabil HK, Zegeye AD, Collick AS, Langan S, MacAlister C, Langendoen EJ, Yitaferu B, Tilahun SA (2015) Improving efficacy of landscape interventions in the (sub) humid Ethiopian highlands by improved understanding of runoff processes. Front Earth Sci 3:1–13. https://doi.org/10.3389/feart.2015.00049

Teramage MT, Onda Y, Kato H, Wakiyama Y, Mizugaki S, Hiramatsu S (2013) The relationship of soil organic carbon to 210Pbex and 137Cs during surface soil erosion in a hillslope forested environment. Geoderma 192:59–67. https://doi.org/10.1016/j.geoderma.2012.08.030

Tian X, Tian P, Zhao G, Gómez JA, Guo J, Mu X, Gao P, Sun W (2023) Sediment source tracing during flood events in the Huangfu River basin in the northern Loess Plateau, China. J Hydrol 620:1–11. https://doi.org/10.1016/j.jhydrol.2023.129540

Tiecher T, Minella JPG, Evrard O, Caner L, Merten GH, Capoane V, Didoné EJ, dos Santos DR (2018) Fingerprinting sediment sources in a large agricultural catchment under no-tillage in Southern Brazil (Conceição River). Land Degrad Dev 29:939–951. https://doi.org/10.1002/ldr.2917

Tilahun SA, Ayana EK, Guzman CD, Dagnew DC, Zegeye AD, Tebebu TY, Yitaferu B, Steenhuis TS (2016) Revisiting storm runoff processes in the upper blue Nile basin: The Debre Mawi watershed. Catena 143: 47–56. https://doi.org/10.1016/j.catena.2016.03.029

Tilahun SA (2012) Observations and modeling of erosion from spatially and temporally distributed sources in the (semi) humid ethiopian highlands. PhD Dessertation Cornel University. https://ecommons.cornell.edu/server/api/core/bitstreams/0910c01a-d385-47ee-994d-aafccbde8ed4/content

Vale S, Swales A, Smith HG, Olsen G, Woodward B (2022) Impacts of tracer type, tracer selection, and source dominance on source apportionment with sediment fingerprinting. Sci Total Environ 831:1–22. https://doi.org/10.1016/j.scitotenv.2022.154832

Vanmaercke M, Poesen J, Broeckx J, Nyssen J (2014) Sediment yield in Africa. Earth-Sci Rev 136:350–368. https://doi.org/10.1016/j.earscirev.2014.06.004

Verheyen D, Diels J, Kissi E, Poesen J (2014) The use of visible and near-infrared reflectance measurements for identifying the source of suspended sediment in rivers and comparison with geochemical fingerprinting. J Soils Sediments 14:1869–1885. https://doi.org/10.1007/s11368-014-0938-9

Wakiyama Y, Onda Y, Yoshimura K, Igarashi Y, Kato H (2019) Land use types control solid wash-off rate and entrainment coefficient of Fukushima-derived 137Cs, and their time

dependence. J Environ Radioact 210:1–12. https://doi.org/10.1016/j.jenvrad.2019.105990
Walling DE (2013) The evolution of sediment source fingerprinting investigations in fluvial systems. J Soils Sediments 13:1658–1675. https://doi.org/10.1007/s11368-013-0767-2
Xu Z, Belmont P, Brahney J, Gellis AC (2022) Sediment source fingerprinting as an aid to large-scale landscape conservation and restoration: A review for the Mississippi River Basin. J Environ Manag 324:1–20. https://doi.org/10.1016/j.jenvman.2022.116260
Yibeltal M, Tsunekawa A, Haregeweyn N, Adgo E, Meshesha DT, Zegeye AD, Andualem T G, Oh SJ, Lee JC, Kang MW, Lee SS (2023) Analyzing the contribution of gully erosion to land degradation in the upper Blue Nile basin, Ethiopia. J Environ Manag 344:1–13. https://doi.org/10.1016/j.jenvman.2023.118378
Zegeye AD, Langendoen EJ, Guzman CD, Dagnew DC, Amare SD, Tilahun SA, Steenhuis, TS (2018) Gullies, a critical link in landscape soil loss: A case study in the subhumid highlands of Ethiopia. Land Degrad Dev 29:1222–1232. https://doi.org/10.1002/ldr.2875

Tables

Table 1 Results of the tracer selection methods

	Conservativeness test	**^{210}Pb-ex**	**^{137}Cs**
Criterion	Mean ± SD	PASS	PASS
	Discriminant power	**^{210}Pb-ex**	**^{137}Cs**
Two-sample Kolmogorov Smirnov test		<0.001***	0.014*

Table 2 Summary of the MixSIAR and BMM model performance metrics based on virtual mixtures (n=21), * indicates mean value.

Sources	ME (%)	RMSE (%)	r^2 (%)	NSE (%)	CRPS* (%)	W50* (%)	Model
Subsoil	5	16	86	73	8.85	21.6	MixSIAR
Topsoil	-5	16	86	73	8.85	21.6	MixSIAR
Subsoil	0	5	99	97	6.68	37.5	BMM
Topsoil	0	5	99	97	6.68	37.5	BMM

Figures

Fig. 1 Photograph showing the expansion of gullying on grazing land (photo taken on 27 June 2023).

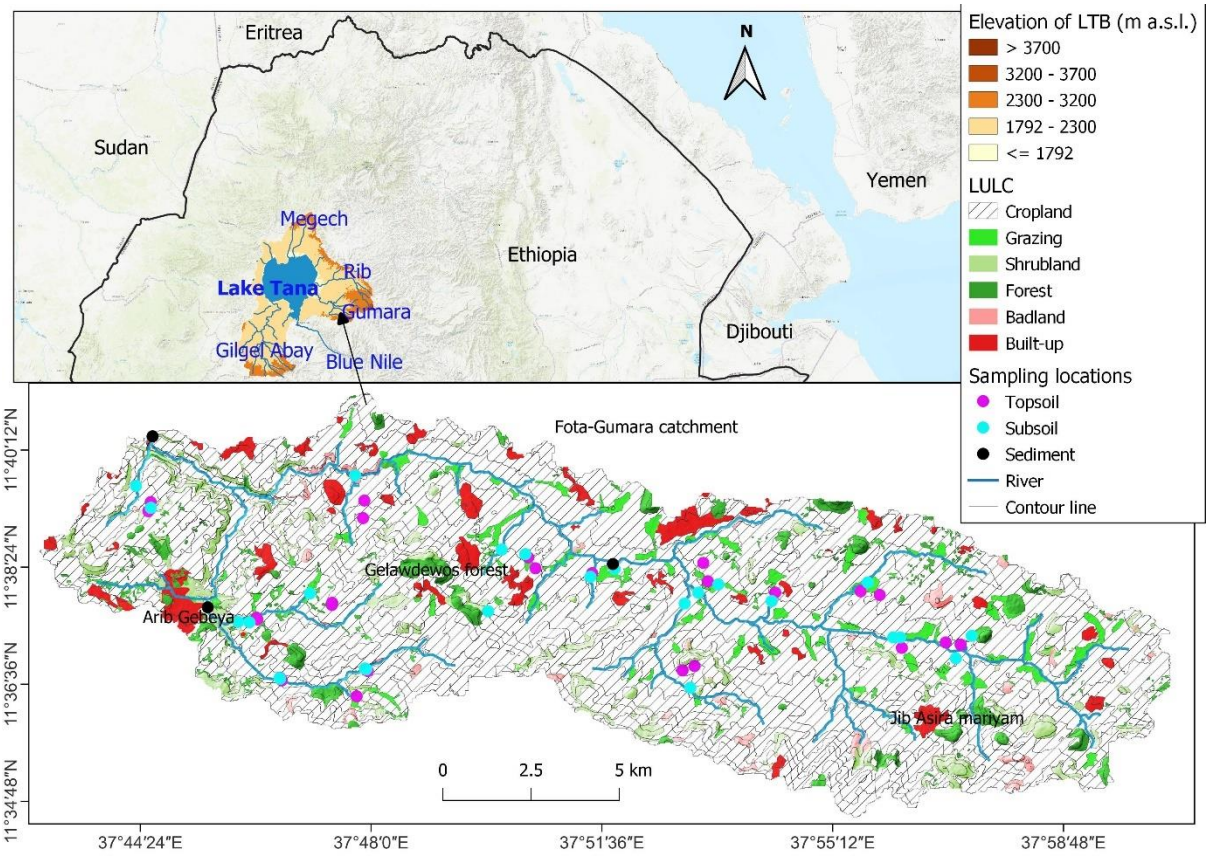

774

775 **Fig. 2** Location of Fota-Gumara Catchment, its main land use types and the sampling locations
776 (topsoil, subsoil and sediment).

777

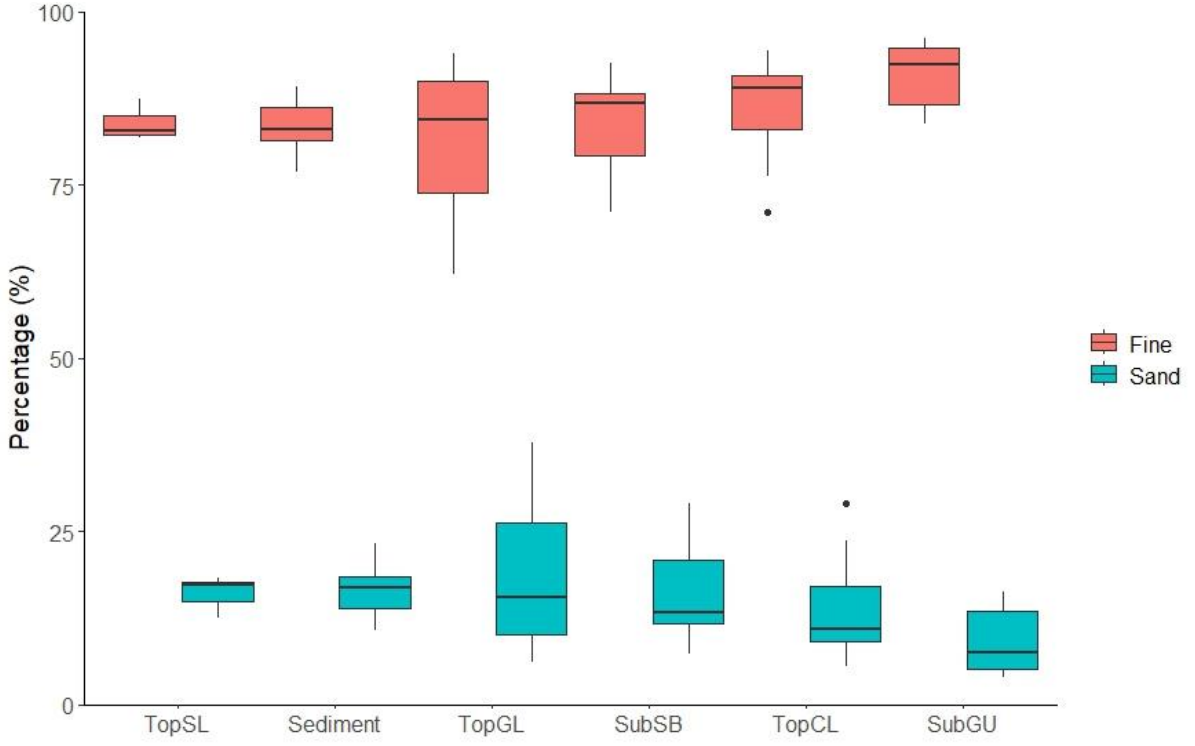

778

779 **Fig. 3** Grain size proportions of the source soil and sediment samples; Fine textures refer to

780 grain sizes below 63 µm, while sand refers to grain sizes between 63 µm and 2,000 µm. TopSL
781 is topsoil from shrubland; TopGL is topsoil from grazing land; SubSB is subsoil from
782 streambank, TopCL is topsoil from cropland, and SubGU is subsoil from gully.

783

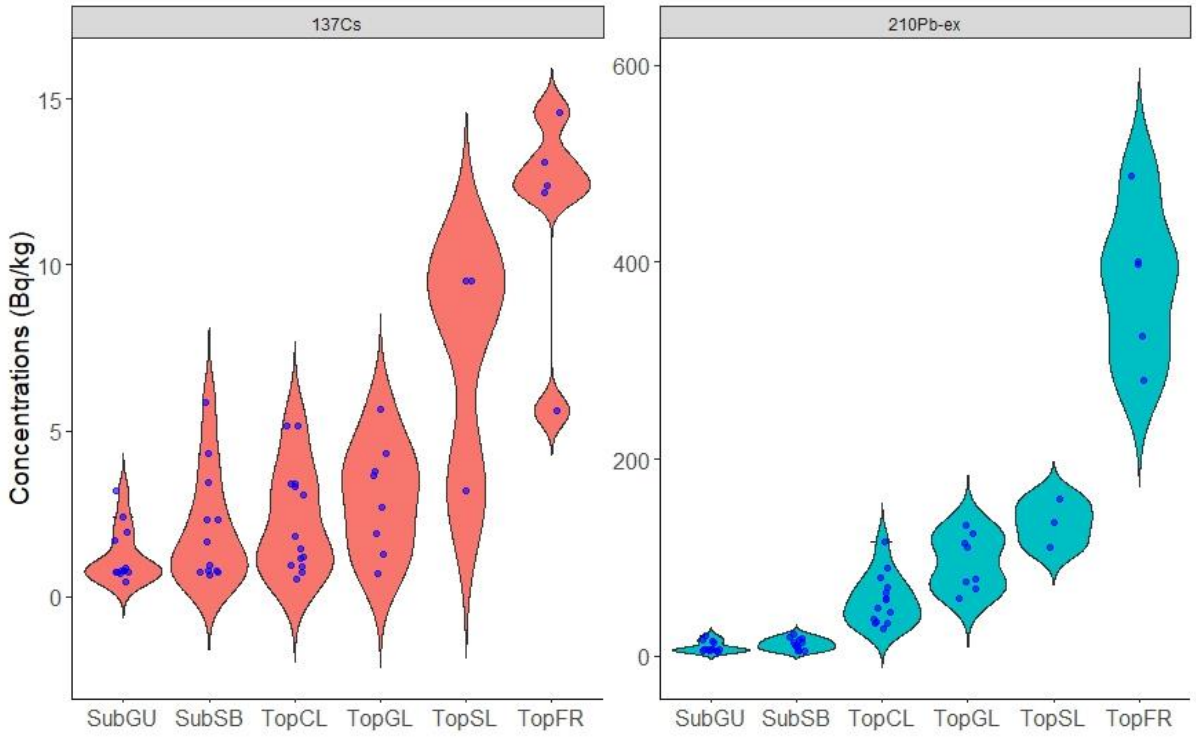

784

785 **Fig. 4** The specific activity of ^{137}Cs and ^{210}Pb-ex for the identified sediment sources and
786 undisturbed forest topsoil. SubGU is subsoil from gully, Sub SB is subsoil from streambank,
787 TopCL is topsoil from cropland, TopGL is topsoil from grazing land, TopSL is topsoil from
788 shrubland and TopFR is topsoil from forestland (*the blue dots are individual data points).*

789

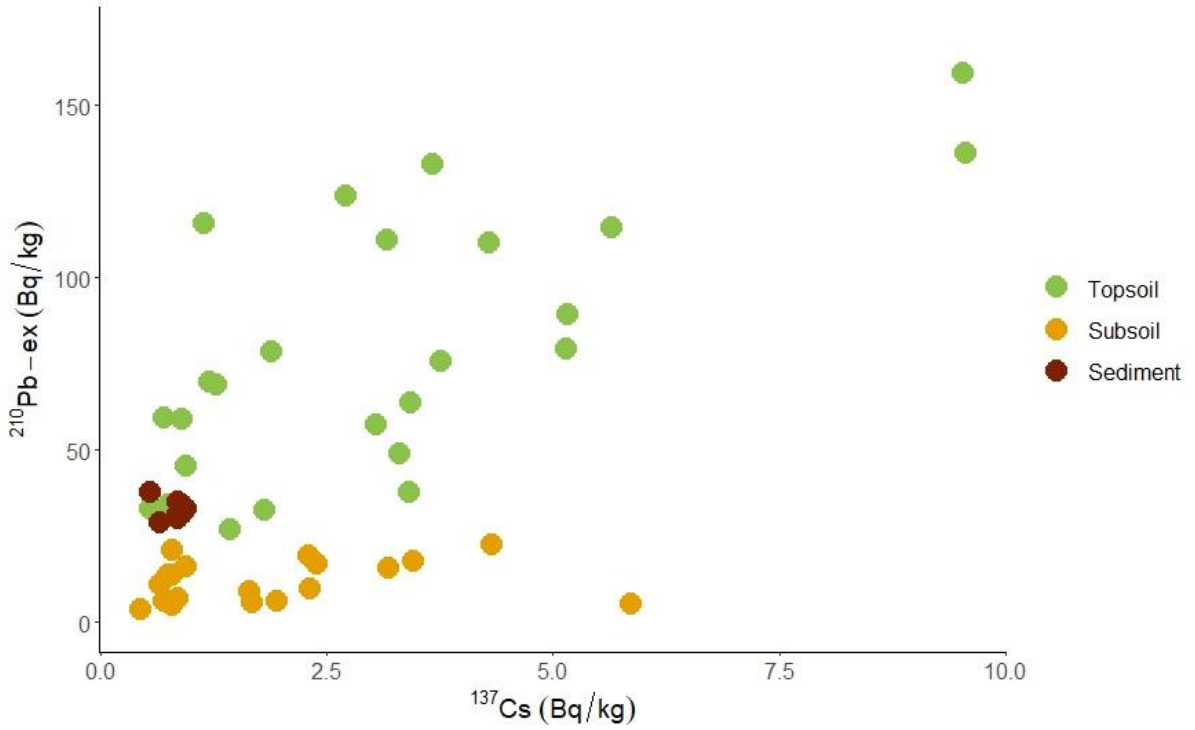

790

791 **Fig. 5** Biplot of radionuclide activities (^{210}Pb-ex & ^{137}Cs) for the different source groups and
792 the lag deposit sediment samples.

793

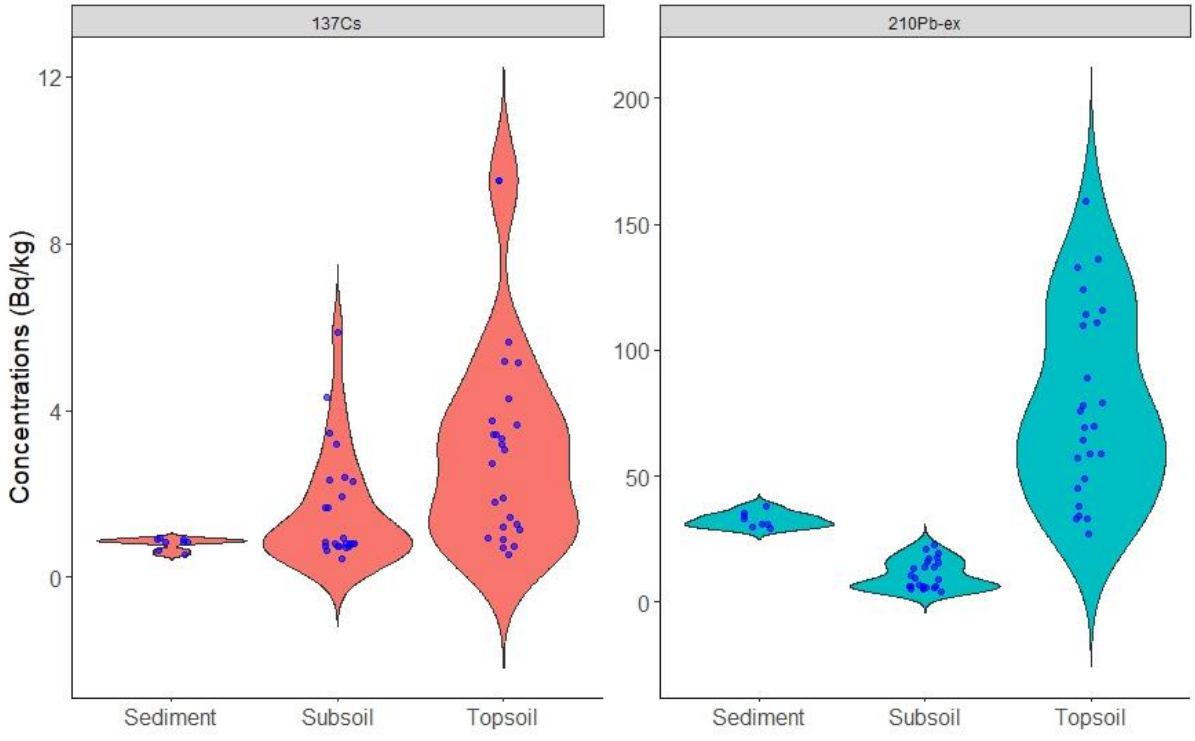

794

795 **Fig. 6** The specific activity of ^{137}Cs and ^{210}Pb-ex for the source soil samples and the target
796 sediment samples (*the blue dots are individual data points*).

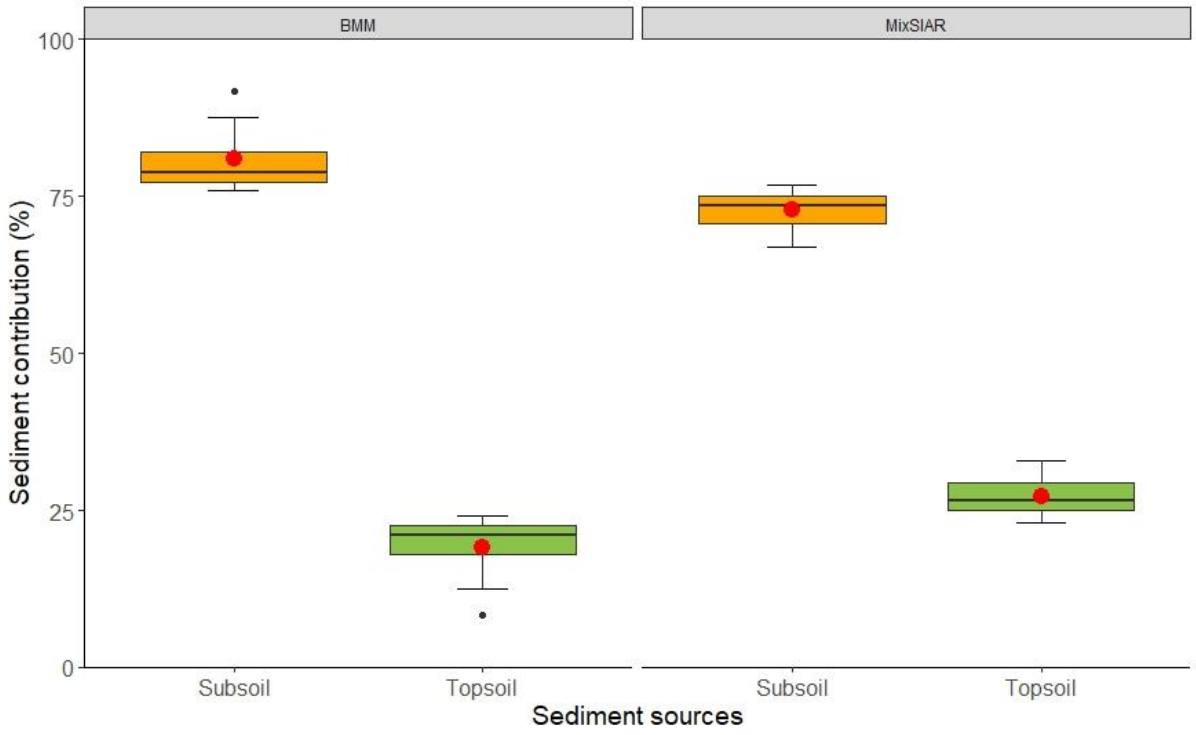

Fig. 7 The median contribution of topsoil and subsoil to the target sediment in BMM and MixSIAR models. "Red dots" indicate mean values.

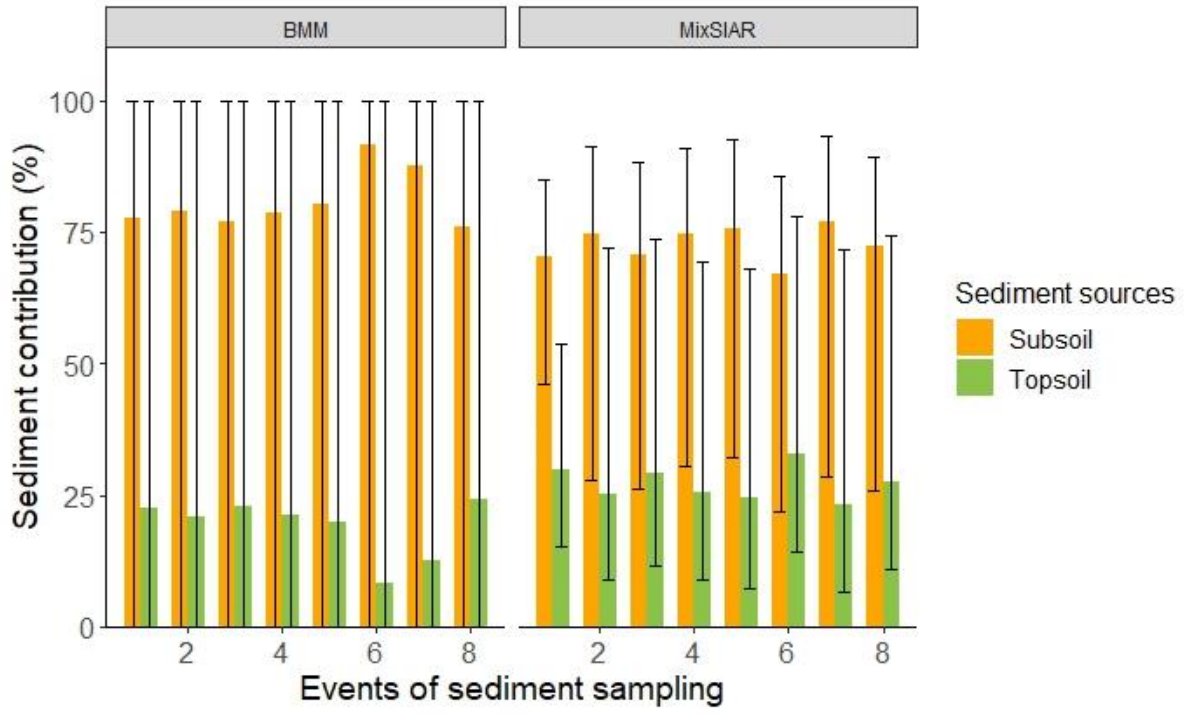

Fig. 8 The median contributions of subsoil and topsoil to sediment mixtures for each event using the BMM and MixSIAR models. Events 1-5 took place at the beginning of the rainy season and events 6-8 occurred at the end of the rainy season. The error bar indicates the 95% credible interval.

Appendix:

Table 3. Sediment source apportionment results in MixSIAR model for the two source types (top-and subsoil)

Sources	Sediments	Mean	SD	Q2.5	Q5	Q25	Q50	Q75	Q95	Q97.5
Subsoil	SD1	0.691	0.098	0.461	0.505	0.634	0.703	0.761	0.83	0.848
Subsoil	SD2	0.707	0.158	0.28	0.381	0.638	0.748	0.817	0.888	0.912
Subsoil	SD3	0.672	0.159	0.263	0.349	0.594	0.707	0.785	0.864	0.884
Subsoil	SD4	0.713	0.151	0.306	0.409	0.648	0.746	0.816	0.891	0.909
Subsoil	SD5	0.722	0.153	0.321	0.408	0.655	0.756	0.829	0.901	0.926
Subsoil	SD6	0.631	0.164	0.219	0.303	0.546	0.67	0.751	0.831	0.857
Subsoil	SD7	0.73	0.158	0.284	0.4	0.666	0.769	0.838	0.914	0.934
Subsoil	SD8	0.682	0.159	0.258	0.349	0.606	0.724	0.793	0.868	0.892
Topsoil	SD1	0.309	0.098	0.152	0.17	0.239	0.297	0.366	0.495	0.539
Topsoil	SD2	0.293	0.158	0.088	0.112	0.183	0.252	0.362	0.619	0.72
Topsoil	SD3	0.328	0.159	0.116	0.136	0.215	0.293	0.406	0.651	0.737
Topsoil	SD4	0.287	0.151	0.091	0.109	0.184	0.254	0.352	0.591	0.694
Topsoil	SD5	0.278	0.153	0.074	0.099	0.171	0.244	0.345	0.592	0.679
Topsoil	SD6	0.369	0.164	0.143	0.169	0.249	0.33	0.454	0.697	0.781
Topsoil	SD7	0.27	0.158	0.066	0.086	0.162	0.231	0.334	0.6	0.716
Topsoil	SD8	0.318	0.159	0.108	0.132	0.207	0.276	0.394	0.651	0.742

Table 4. Sediment source apportionment results in BMM model for the two source types (top- and subsoil)

Sources	Sediments	Mean	SD	Q2.5	Q5	Q25	Q50	Q75	Q95	Q97.5
Subsoil	SD1	0.649	0.347	0.001	0.001	0.381	0.775	0.951	0.999	0.999
Subsoil	SD2	0.673	0.331	0.001	0.001	0.458	0.79	0.96	0.999	0.999
Subsoil	SD3	0.657	0.331	0.001	0.001	0.423	0.77	0.945	0.999	0.999
Subsoil	SD4	0.681	0.322	0.001	0.001	0.499	0.787	0.953	0.999	0.999
Subsoil	SD5	0.691	0.319	0.001	0.001	0.512	0.802	0.962	0.999	0.999
Subsoil	SD6	0.681	0.402	0.001	0.001	0.286	0.917	0.999	0.999	0.999
Subsoil	SD7	0.713	0.349	0.001	0.001	0.539	0.875	0.999	0.999	0.999
Subsoil	SD8	0.654	0.327	0.001	0.001	0.434	0.759	0.938	0.999	0.999
Topsoil	SD1	0.351	0.347	0.001	0.001	0.049	0.225	0.619	0.999	0.999
Topsoil	SD2	0.327	0.331	0.001	0.001	0.04	0.21	0.542	0.999	0.999
Topsoil	SD3	0.343	0.331	0.001	0.001	0.055	0.23	0.577	0.999	0.999
Topsoil	SD4	0.319	0.322	0.001	0.001	0.047	0.213	0.501	0.999	0.999
Topsoil	SD5	0.309	0.319	0.001	0.001	0.038	0.198	0.488	0.999	0.999
Topsoil	SD6	0.319	0.402	0.001	0.001	0.001	0.083	0.714	0.999	0.999
Topsoil	SD7	0.287	0.349	0.001	0.001	0.001	0.125	0.461	0.999	0.999
Topsoil	SD8	0.346	0.327	0.001	0.001	0.062	0.241	0.566	0.999	0.999